

Liquid-Film Instabilities in Confined Geometries

D. D. Awschalom, J. Warnock, and M. W. Shafer

IBM Watson Research Center, Yorktown Heights, New York 10598

(Received 10 March 1986)

Sol-gel methods combined with specific thermal treatments were used to fabricate porous glasses with extremely uniform pore diameters and high internal surface areas. Low-temperature adsorption isotherm measurements reveal the dynamic and thermodynamic stability limits of the liquid films as a function of evolving pore diameter. Contrary to classical predictions, the results are in remarkable agreement with a universal hydrodynamic theory of film behavior which includes substrate interactions.

PACS numbers: 68.45.-v, 67.40.Hf, 82.70.Gg

The physics of liquid films adsorbed onto porous substrates and the properties of fluids restricted within porous media has received considerable attention from a broad range of disciplines in the science community. In particular, a variety of low-temperature physics experiments have been conducted in order to study the behavior of liquid ^4He as it evolves from monolayer films up to and including "bulk" coverage. A number of different porous substrates have been employed for these measurements including packed powders,¹ Nucleopore filters,² and Vycor glass.³ In order to understand the importance of capillary condensation in many of these experiments, a theory is required that considers the thermodynamics and dynamics of liquid films in porous media. One such theory which has been advanced by Cole and Saam⁴ (CS) contains a great deal of predictive power concerning the stability of liquid films in cylindrical pores. Here we report a series of experiments which, for the first time, directly test the theoretical predictions of this theory with rather remarkable results.

The CS theory^{4,5} considers volume and surface excitations of adsorbed liquid films in partially and completely filled cylindrical cavities by calculating the film's hydrodynamic excitation spectrum and the thermodynamics of adsorption. As the layer of adsorbed film thickens in a pore of radius R [Fig. 1(a)], normal mode excitations become sensitive to the geometry and it is concluded that an instability will arise, because it becomes energetically favorable to partially fill the pore in order to reduce the surface area. The radius of dynamic instability, a_c , is calculated from the excitation spectrum as well as being derived from thermodynamic considerations alone. Most importantly, one may calculate its numerical value as a function of film thickness and substrate parameters,⁴ hence obtaining a quantitative description of the liquid behavior as it evolves from a thick film to the capillary-condensed state. Conversely, during the emptying of a full pore there exists a similar radius, a_m , at which the film is metastable relative to the partially filled pore, as

it becomes energetically favorable for the system to assume a layered configuration. In terms of the scaling parameter R_0 , where $R_0 = (3\pi\alpha\rho/\sigma M)^{1/2}$, the instability criterion a_c can be written in dimensionless units as⁴

$$\begin{aligned} (R/R_0)^2 \\ = y_c^2(1-y_c^2)^{-5/2} P_{3/2}^1((1+y_c^2)/(1-y_c^2)), \end{aligned} \quad (1)$$

and a_m as

$$2a_m^{-2} \int_0^{a_m} dr rU(r) = U(a_m) + \sigma M/a_m\rho. \quad (2)$$

Here α and $U(r)$ are the gas-substrate van der Waals interaction coefficient⁶ and potential,⁷ ρ the liquid density, σ the surface tension, M the molecular weight, R the pore radius, $P_{3/2}^1$ an associated Legendre

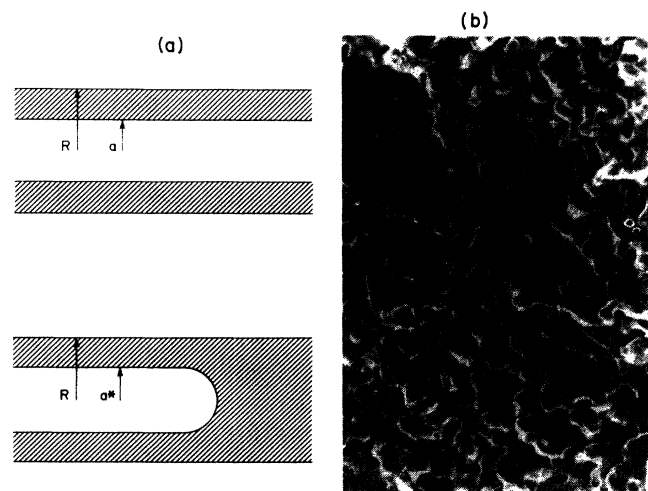


FIG. 1. (a) Schematic drawing of liquid in a pore, both in an adsorbed and partially filled geometry. $a^* = a_c$ during filling and $= a_m$ during emptying. (b) Medium-resolution transmission-electron-microscopy photograph of sol-gel glass, where the solid scale line indicates 1350 Å.

function, and $y_c = a_c/R$. Hence we are provided with a definite prediction of the limits of stability, a_c and a_m , in which both the functional forms and absolute values of the film thicknesses are contained. Note that these are universal predictions and there is no explicit temperature dependence contained in the equations.

Apart from some theoretical analyses of early data of ^4He adsorbed on Vycor glass^{5,8} and more recently in Nucleopore filter,⁹ very little quantitative information about film instabilities in varying pore geometries is available. Earlier experiments had been forced to select one of the few different available porous substrates which are reasonably well characterized in terms of pore uniformity and porosity.² Moreover, complications arise when one attempts to analyze the existing data using the classical Kelvin equation of capillary condensation,¹⁰

$$\ln(p/p_0) = - (2M\sigma/r\rho k_B T) \cos\theta, \quad (3)$$

where p is the vapor pressure, p_0 the saturated vapor pressure, T the temperature of the adsorbed liquid, and θ the angle of contact between the liquid and capillary walls. For example, it is extremely difficult to determine the required contact angle of the fluid against the substrate in the case of a porous solid. In addition, the classical arguments attempt to reconcile the observed hysteresis in porous media with either structural changes in the pores themselves¹¹ or differing shapes of the meniscus during adsorption and desorption.¹⁰ Finally, the Kelvin equation completely omits van der Waals forces which often dominate the physics of thin films.¹² Despite important experimental and theoretical implications, the major features of the CS theory remain largely untested. However, with the new porous-glassmaking techniques described below, it is possible to control the pore geometry in order to yield samples with a continuous range of pore diameters, thereby providing excellent hosts in which to test systematically the conditions of film instability.

The glasses used in this study are essentially pure silica prepared by the sol-gel¹³ technique and then carefully dehydrated to porous xerogels at temperatures between 300 and 900°C. In particular, two types of "gels" were necessary to obtain the broad range of pore diameters required, i.e., < 20 to 380 Å. The first type were formed by the hydrolysis of the methoxide or ethoxide of silica. In general the maximum pore size obtainable from the alkoxide gels was in the 100–120-Å range. The second type involved the gelling of LUDOX¹⁴ with K_2SiO_3 and subsequent removal of the alkali by acid leaching.¹⁵ The pore size for both methods was highly dependent on the $\text{SiO}_2/\text{H}_2\text{O}$ or $\text{SiO}_2/\text{K}_2\text{O}$ ratio as well as the firing temperatures. In both cases the pore size was shown to increase with temperature up to the point of densification via viscous sintering (850–900°C).

Details of the final glass morphology may be seen through transmission electron microscopy¹⁶ as shown in Fig. 1(b). This picture is only one of a pair of stereoscopic photographs which, when properly viewed, gives depth perception to the image and shows the pores to be tortuous and highly interconnected. Analysis of these photographs reveals a pore geometry with an average pore length to diameter ratio of approximately 7:1. The pore size distribution as well as the surface area could be determined by mercury porosimetry as seen in Fig. 2(a). Even in the case of large pores, the distribution of pore diameters is extremely narrow with over 96% of the pores having radii within 5% of the average radius in the best samples. Typical glasses formed by this process have a porosity of approximately 70% and a surface area of several hundred square meters per gram. The samples were carefully cleaned in several stages after firing including boiling in ethanol, hydrogen peroxide, and distilled water. Afterwards the glasses were desiccated and vacuum pumped to remove any foreign physisorbed contaminants. A complete description of the gel-glass preparation and characterization will be presented elsewhere.¹⁷

The glass samples were evacuated in a closed copper cell and placed inside a variable temperature cryostat held at $T = 90$ K, the boiling point of liquid oxygen. A few millimeters of helium exchange gas was added before each run to insure thermal equilibrium inside and around the glass sample with the surrounding copper. A typical oxygen adsorption-desorption measurement is shown in Fig. 2(b), taking approximately 36 h per scan. Note that analysis of this measurement also serves as a check of the porosimetry data for pore size and distribution, and internal surface area.

Referring to Fig. 2(b), the initial part of the adsorption curve is characteristic of a vapor as it forms several adsorbed layers on the solid. This may be demonstrated by Brunauer-Emmett-Teller analysis¹⁸ as shown in the inset. For a sufficiently thick film of radius a_c the adsorbate becomes unstable, capillary condensation occurs at point A, and the amount of added liquid increases until all pores are just filled at point B. Finally further condensation causes the menisci to flatten until they are planar, the vapor is fully saturated, and bulk condensation can occur. During desorption, the menisci are pulled down with decreasing pressure until the liquid attempts to minimize its total free energy by jumping from its metastable state at point C to that of a thick adsorbed film of radius a_m at point D. The very sharp desorption knee indicates the high degree of pore uniformity within the sample and is commensurate with the narrow pore size distribution seen in porosimetry data.

The sharp features of the isotherm curves allow the points of film instability to be directly read from the

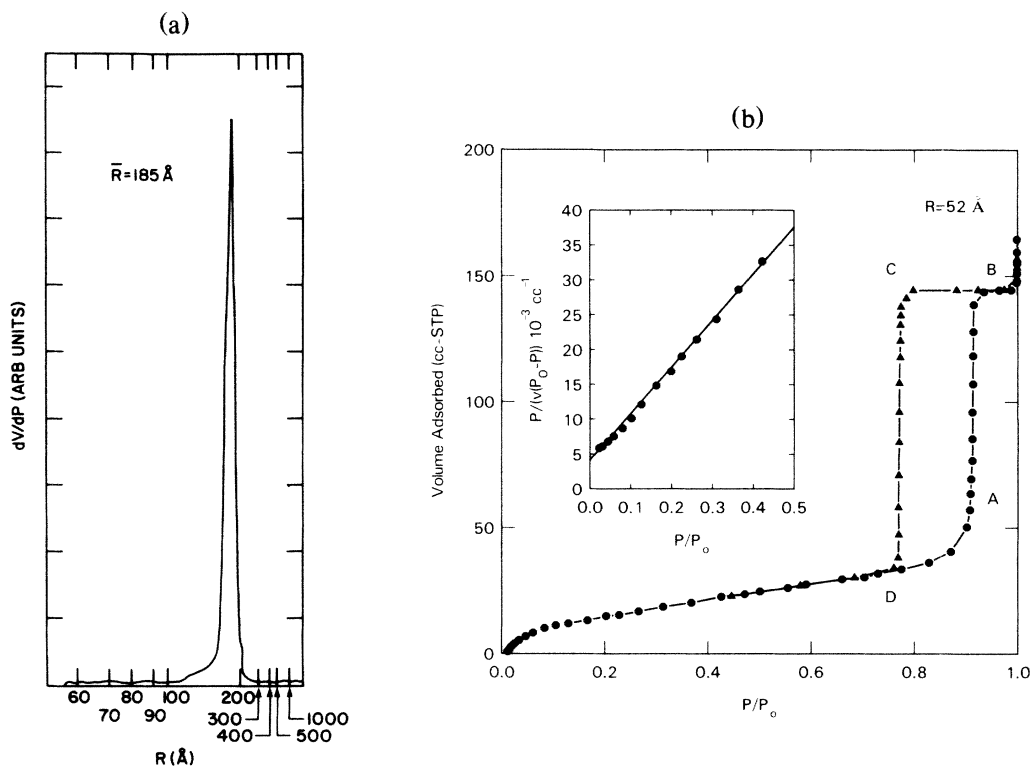


FIG. 2. (a) Large-pore porosimetry data yielding a surface area of $61 \text{ m}^2/\text{g}$ and a porosity of 52%. (b) Medium-pore liquid-oxygen adsorption isotherm at $T = 89.50 \text{ K}$, with inset of Brunauer-Emmett-Teller analysis.

data. The radius of film instability a_c is obtained from the fraction of the full pore volume taken at the point of infinite derivative during adsorption. Similarly, the radius a_m is obtained from the fractional volume taken at the bottom of the vertical desorption branch of the isotherm. Adsorption-desorption measurements were performed for a number of samples ranging over an order of magnitude in pore diameters, and the tabulated radii of instability were then plotted in Fig. 3. The scaling for silica gels is obtained by calculation of $R_0 = 8.84 \text{ \AA}$ for oxygen on silica with use of the substrate van der Waals energy⁶ $\alpha = 0.32 \text{ eV \AA}^3$. The solid curves represent the theoretical predictions of CS theory reproduced from Ref. 4, based upon the numerical calculations of Eqs. (1) and (2) above, and are in excellent agreement with the experimental results. Without substrate interactions, the CS theory reduces to the classical Kelvin relation [Eq. (3)] for capillary condensation in porous media which is shown as the dashed curve in Fig. 3. The dotted curve displays a common description of the classical desorption limit assuming a hemispherical liquid meniscus radius.¹⁰ Clearly our results show that both the functional form and magnitude of the CS predictions are valid in marked contrast to the classical theory. In addition, two isotherm measurements were performed with krypton at $T = 118.0 \text{ K}$. By calculation of $R_0 = 17.9 \text{ \AA}$

with⁶ $\alpha = 0.55 \text{ eV \AA}^3$, the data are also shown in Fig. 3 with good theoretical agreement.

Hysteresis in porous media has often been attributed to nonuniform pore geometries where the film radius of curvature depends on whether liquid is being added or removed. Under less stringent growth conditions porous glasses with wide pore distributions may be obtained, and measurements from these materials showed rounded desorption knees, canted desorption isotherms, and an absence of sharp capillary effects. As the sample pore size distribution narrows, the hysteretic region sharpens and appears to move towards the predicted theoretical limits.¹⁶ Thus our data suggest that hysteresis is in fact a fundamental consequence of hydrodynamic instabilities governed by substrate forces. Sound measurements of ^4He films in Nucleopore filter² have also shown hysteresis whose width was in qualitative agreement with the CS theory and has been attributed to capillary condensation.

In conclusion, we have successfully used the sol-gel technique to fabricate extremely uniform diameter porous glasses with high porosity. High-resolution stereoscopic transmission-electron-microscopy photographs and mercury porosimetry data demonstrate the presence of a well-defined restricting geometry. The extensive isotherm measurements made possible as a result of the existence of these materials reveal sharp

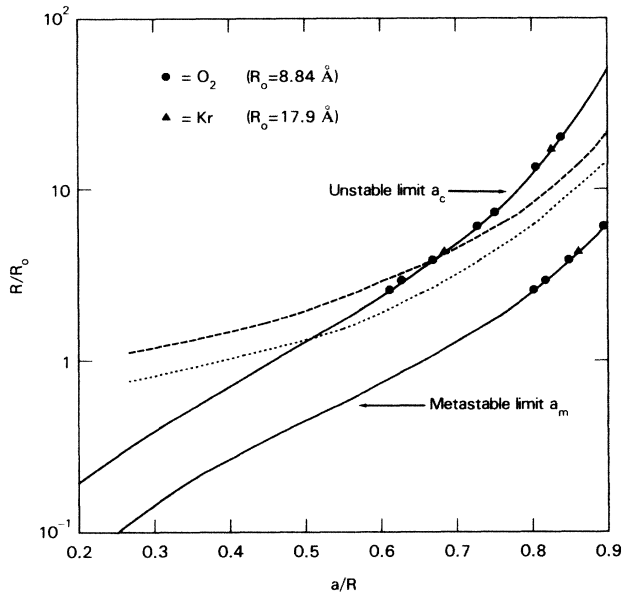


FIG. 3. Comparison of CS theory with experimental results. The solid lines are reproduced from Ref. 4 and show the CS predictions. The dashed line is the classical Kelvin relation with Brunauer-Emmett-Teller layering, and the dotted line the classical desorption limit for a hemispherical-meniscus model. The filled circles are the data from oxygen isotherms and the filled triangles are from krypton isotherms.

hysteretic behavior between the point of capillary condensation and pore emptying. The liquid film instabilities, seen both in oxygen and krypton, are successfully predicted by the hydrodynamic theory of Cole and Saam both in functional form and in absolute magnitude over a wide range of pore diameters. Contrary to classical theories, these results imply that van der Waals forces are important in determining the stability points of liquid films and cannot be ignored in the study of porous media. Hysteretic behavior arises as a natural consequence of surface interactions and can be explained without additional assumptions about the pore structure or on the detailed shapes of the liquid menisci. Substrate effects are always present but often hidden as a result of fluid behavior in ill-defined geometries.

We would like to thank Milton Cole for helpful dis-

cussions and theoretical calculations, and R. Figat for technical assistance in preparing the gel glasses.

¹G. A. Williams, R. Rosenbaum, and I. Rudnick, *Phys. Rev. Lett.* **42**, 1282 (1979).

²J. M. Valles, Jr., D. T. Smith, and R. B. Hallock, *Phys. Rev. Lett.* **54**, 1528 (1985).

³J. E. Berthold, D. J. Bishop, and J. D. Reppy, *Phys. Rev. Lett.* **39**, 348 (1977).

⁴M. W. Cole and W. F. Saam, *Phys. Rev. Lett.* **32**, 985 (1974).

⁵W. F. Saam and M. W. Cole, *Phys. Rev. B* **11**, 1086 (1975).

⁶S. Rauber, J. R. Klein, M. W. Cole, and L. W. Bruch, *Surf. Sci.* **123**, 173 (1982); G. Vidali and M. W. Cole, *Surf. Sci.* **110**, 10 (1981).

⁷I. E. Dzyaloshinski, E. M. Lifshitz, and I. P. Pitaevski, *Adv. Phys.* **10**, 165 (1961).

⁸D. F. Brewer and D. C. Champeney, *Proc. Phys. Soc. London* **79**, 885 (1962).

⁹T. P. Chen, M. J. DiPirro, A. A. Gaeta, and F. M. Gasparini, *J. Low. Temp. Phys.* **26**, 927 (1977); see also S. M. Cohen, R. A. Guyer, and J. Machta, *Phys. Rev. B* (to be published). This theoretical work analyzes the data of Ref. 2 with a method similar to that of Cole and Saam, comparing grand potentials instead of energies.

¹⁰S. J. Gregg and K. S. W. Sing, *Adsorption, Surface Area, and Porosity* (Academic, New York, 1967), Chaps. 3 and 4.

¹¹R. Defay and I. Prigogine, *Surface Tension and Adsorption* (Longmans, London, 1966), pp. 225–226.

¹²C. E. Bartosch and S. Gregory, *Phys. Rev. Lett.* **54**, 2513 (1985).

¹³See, for example, *Ultrastructure Processing of Glasses, Ceramics, and Composites*, edited by L. Hench and D. Ulrich (Wiley, New York, 1984); M. W. Shafer, V. Castano, W. Krakow, R. Figat, and G. Ruben, in *Materials Research Society Symposia Proceedings*, Palo Alto, California, 1986 (to be published).

¹⁴Trade name for DuPont colloidal silica.

¹⁵R. D. Sharp, *J. Colloid Interface Sci.* **3**, 63 (1976).

¹⁶G. Ruben and M. W. Shafer, in *Materials Research Society Symposia Proceedings*, Palo Alto, California, 1986 (to be published).

¹⁷M. W. Shafer, D. D. Awschalom, and J. Warnock, to be published.

¹⁸S. Brunauer, P. H. Emmett, and E. Teller, *J. Am. Chem. Soc.* **60**, 309 (1938).

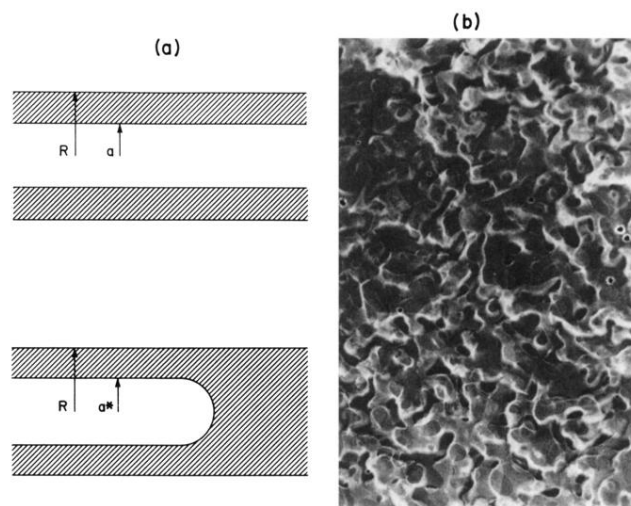


FIG. 1. (a) Schematic drawing of liquid in a pore, both in an adsorbed and partially filled geometry. $a^* = a_c$ during filling and $= a_m$ during emptying. (b) Medium-resolution transmission-electron-microscopy photograph of sol-gel glass, where the solid scale line indicates 1350 Å.